Forms of zinc accumulated in the hyperaccumulator Arabidopsis halleri

Geraldine Sarret, Pierre Saumitou-Laprade, Valerie Bert, Olivier Proux, Jean-Louis Hazemann, Agnes Traverse, Matthew A. Marcus, Alain Manceau

Sarret G., Saumitou-Laprade P., Bert V., Proux O., Hazemann J. L., Traverse A., Marcus M. A. and Manceau A., 2002, Forms of zinc accumulated in the hyperaccumulator *Arabidopsis halleri*. *Plant Physiol*., 130, 1815-1826.

Forms of Zn Accumulated in the Hyperaccumulator *Arabidopsis halleri* [a]

Géraldine Sarret[1*], Pierre Saumitou-Laprade[2], Valérie Bert[2, b], Olivier Proux[3], Jean-Louis Hazemann[3], Agnès Traverse[4], Matthew A. Marcus[5], and Alain Manceau[1]

1 - Environmental Geochemistry Group, LGIT, University of Grenoble and CNRS, BP 53, 38041 Grenoble Cedex 9, France;

2 - Laboratoire de Génétique et Evolution des Populations Végétales, UPRESA-CNRS 8016 FR CNRS CNRS-1818, Bât SN2, Université de Lille1, 59655 Villeneuve d'Ascq Cedex, France;

3 - Laboratoire de Cristallographie, CNRS, 25 avenue des Martyrs, BP 166, 38042 Grenoble Cedex 9, France;

4 - Laboratoire pour l'Utilisation du Rayonnement Electromagnétique, Bât 209D Centre Universitaire, BP 34, 91898 Orsay Cedex, France;

5 - ALS, Berkeley Lab, MS 6-2100, Berkeley, CA 94720, USA.

FOOTNOTES

[a] This research was supported by the CNRS, "Programme Environnement, Vie et Société" (grant n° 00N55) and by the Nord-Pas-de-Calais Region, "Programme de Recherches Concertées".

[b] Present address: Laboratoire de Physiologie et de Génétique Moléculaire des Plantes, Campus Plaine, ULB, CP 242, Bd du Triomphe, 1050 Bruxelles, Belgium.

*Corresponding author; e-mail geraldine.sarret@ujf-grenoble.fr; fax 33-4-76-82-81-01.

ABSTRACT

The chemical forms of zinc in the Zn tolerant and hyperaccumulator *Arabidopsis halleri* and in the non-tolerant and non-accumulator *Arabidopsis lyrata* ssp. *petraea* were determined at the molecular level by combining chemical analyses, extended X-ray absorption spectroscopy (EXAFS), synchrotron-based X-ray microfluorescence (µSXRF) and µEXAFS. Plants were grown in hydroponics with various Zn concentrations, and *A. halleri* specimens growing naturally in a contaminated site were also collected. Zn speciation in *A. halleri* was independent of the origin of the plants (contaminated or non-contaminated) and Zn exposure. In aerial parts, Zn was predominantly octahedrally coordinated and complexed to malate. A secondary organic species was identified in the bases of the trichomes, which contained elevated Zn concentrations, and in which Zn was tetrahedrally coordinated and complexed to carboxyl and/or hydroxyl functional groups. This species was detected thanks to the good resolution and sensitivity of µSXRF and µEXAFS. In the roots of *A. halleri* grown in hydroponics, Zn phosphate was the only species detected, and is believed to result from chemical precipitation on the root surface. In the roots of *A. halleri* grown on the contaminated soil, Zn was distributed in Zn malate, Zn citrate, and Zn phosphate. Zn phosphate was present in both the roots and aerial part of *A. lyrata* ssp. *petraea*. This study illustrates the complementarity of bulk and spatially resolved techniques, allowing the identification of (1) the predominant chemical forms of the metal, and (2) the minor forms present in particular cells, both types of information being essential for a better understanding of the bioaccumulation processes.

INTRODUCTION

Metal tolerant plants have the ability to survive and reproduce on soils containing high concentrations of metals in forms that are toxic or inimical to other plants (Macnair & Baker, 1994). Metal hyperaccumulating plants have the additional property of storing large amounts of metals in their aerial parts, more than typically 10000 µg g^{-1} (d. w.) for Zn (Baker, 1990). This characteristic makes hyperaccumulators highly suitable for phytoremediation, a soft method in which plants are used for the cleanup of metal-polluted soils (Books, 1998, Baker *et al.*, 2000). The genetics and the biochemical processes involved in metal uptake, transport, and storage by hyperaccumulating plants are still poorly understood, although this basic information is fundamental for the improvement of the technique (Van Der Lelie *et al.*, 2001). Zinc is one of the most important metal contaminant in industrialized countries (Nriagu and Pacyna, 1988), and numerous studies have been conducted on the species *Thalspi caerulescens* (Vazquez *et al.*, 1992, Vazquez *et al.*, 1994, Pollard & Baker, 1996, Lasat *et al.*, 1998, Küpper *et al.*, 1999, Salt *et al.*, 1999, Frey *et al.*, 2000, Lasat *et al.*, 2000, Assunçaõ *et al.*, 2001) and, to a lesser extent, on *Arabidopsis halleri* (Macnair et al., 1999, Bert et al., 2000, Küpper *et al.*, 2000, Zhao *et al.*, 2000). This latter species is of particular interest because it is one of the closest relatives to *A. thaliana* (Koch *et al.*, 2001), whose genome is entirely sequenced (Kaul & al., 2000, Meinke *et al.*, 1998). This information, together with the huge amount of literature available on *A. thaliana*, should facilitate our understanding of metal tolerance and hyperaccumulation in *A. halleri*.

A. halleri is a pseudo-metallophyte, which means that it is found both in polluted and non-polluted areas. It is known as a Zn hyperaccumulator, but recent studies showed that it can also hyperaccumulate Cd (Dahmani-Muller *et al.*, 2000, Küpper *et al.*, 2000, Bert *et al.*, in press). By analyzing F2 progenies produced by interspecific crosses between *A. halleri* and the non-tolerant and non-hyperaccumulating *Arabidopsis lyrata* ssp. *petraea*, Macnair *et al.* (1999) demonstrated

that Zn tolerance and Zn hyperaccumulation are two genetically independent characters. Moreover, by comparing Zn tolerance and Zn hyperaccumulation abilities of several populations of *A. halleri* originating from contaminated and uncontaminated areas, Bert *et al.* (2000) showed that both characters are constitutive properties of the species, but that populations from uncontaminated sites are slightly less Zn tolerant but exhibit higher Zn accumulation rates than populations from contaminated sites.

Recent studies by scanning electron microscopy and energy dispersive X-ray microanalysis (SEM-EDX) documented the cellular distribution of Zn in the tissues of *A. halleri* grown in hydroponics (Küpper *et al.*, 2000, Zhao *et al.*, 2000). In the leaves, Zn was mostly sequestered in the base of the trichomes and in mesophylle cells. Trichomes are epidermal hairs present at the surface of plant leaves, and their function can be as diverse as the exudation of various molecules, the protection against the wind and sunlight, or the storage of metals (Rodriguez *et al*., 1983). The chemical form of Zn accumulated in the trichomes and in mesophylle cells of *A. halleri* was not determined. Another study on *A. halleri* grown in Zn-containing hydroponics showed a correlation between the concentration of Zn and the concentration of P, citric, and malic acid in the roots (Zhao *et al.*, 2000). The Zn-P correlation was attributed to Zn phosphate precipitates at the root surface. No Zn correlation with P or organic acids was found in the leaves.

In hydroponic studies, the nutrient solution used is generally devoid of Si because this element is not considered essential to plants (Epstein, 1999). However, some Zn-containing silicate aggregates were observed in the cytoplasm and in pinocytotic vesicles of *A. halleri* leaves grown on polluted soils, suggesting that Zn was transiently present as Zn silicate in the cytoplasm, before being translocated and stored in the vacuoles in an undetermined form (Neumann & zur-Nieden, 2001).

The aim of this study is to address several open questions concerning the mechanisms of Zn tolerance and hyperaccumulation in *A. halleri*. First, what are the accumulation forms of Zn in the roots and in the aerial parts of *A. halleri*, and are they specific to this species or common to a non-tolerant and non-hyperaccumulating *Arabidopsis* species such as *A. lyrata* ssp. *petraea*? Second, within *A. halleri* species, do Zn accumulation forms depend on the origin of the plant (contaminated or non-contaminated)? Third, does the nature of the growing medium (soil *vs.* hydroponics) and Zn concentration in the nutrient solution influence Zn speciation in the plant? To address these questions, two populations of *Arabidopsis halleri*, one originating from a contaminated site (*A. h.* -C) and one from a non-contaminated site (*A. h.* -NC), as well as a non-tolerant and non-hyperaccumulating species, *Arabidopsis lyrata* ssp. *petraea* (*A. l.*) (Macnair *et al.*, 1999), were grown in hydroponics at various Zn levels. In addition, natural specimens of *A. halleri* growing in a contaminated soil were collected. The chemical form of Zn in the roots and in the aerial parts of the plants was studied by Zn K-edge extended X-ray absorption fine structure (EXAFS) spectroscopy on powder samples, and results were interpreted in light of elemental and organic acids concentrations. The localization and speciation of Zn in the leaves of *A. halleri* was also investigated at the micron scale by synchrotron-based X-ray microfluorescence (μSXRF) and μEXAFS spectroscopy.

RESULTS

Elemental and organic acids concentrations

Total concentrations of Zn, P and organic acids in the aerial parts and in the roots of the plants are presented in Table I. For the two populations of *A. halleri* grown in hydroponics, Zn concentrations increase with Zn exposure. The transfer coefficient ($[Zn]_{aerial\ parts}/[Zn]_{roots}$) is always close to or less than 1, which is unexpected for an hyperaccumulating species. Such a low

transfer coefficient was already observed in hydroponic experiments (Küpper *et al.*, 2000), and is attributed to the precipitation of Zn phosphates on the root surface. Indeed, Figure 1 shows that P and Zn concentration are clearly correlated in the roots of hydroponic plants (group B on Fig. 1), but not in the other samples (group A on Fig. 1, including the aerial parts of all plants and the roots of *A. h*. grown on a contaminated soil). Moreover, *A. h*. grown on a contaminated soil presents a higher transfer coefficient than hydroponic plants (1.5), which is consistent with a chemical precipitation of Zn phosphate on hydroponic roots only. We shall see below that this interpretation is also supported by EXAFS results.

For a given Zn concentration in solution (250 or 100 µM Zn), the population from non-contaminated origin (*A. h*. -NC) accumulates more Zn in its aerial parts than that from contaminated origin (*A. h*. -C), which confirms previous observations made at lower Zn concentration (50 µM, Bert *et al*., 2000). The higher aerial Zn accumulation in *A. h*. -NC was not accompanied by visible toxicity signs, such as chlorosis or low growth. *A. lyrata* ssp. *petraea* (*A. l.*) grown in 10 µM Zn exhibits a very low transfer coefficient (0.1), as expected for a non-hyperaccumulating species.

The concentrations of the three organic acids most often inferred to bind metals (citrate, malate and oxalate) (Verkleij & Schat, 1989, Streit & Stumm, 1993, Brooks, 1998) were also measured, and compared to total Zn concentrations (Table I). In the roots, for all, but two, samples, the organic acid/Zn molar ratios are lower than 1 (Table I, Figure 2). Moreover, the sum of the three organic acids/Zn ratio is lower than one for all, but three, samples. Thus, these ligands are not concentrated enough to bind all Zn atoms present in the roots. In the aerial parts, the malate/Zn molar ratio is higher than 1 in all the samples, whereas citrate/Zn and oxalate/Zn ratios are lower than 1. Thus, malate could bind all Zn atoms present in the aerial parts by forming 1:1 complexes (the predominant complex if we consider a solution containing equivalent

concentrations of Zn and malate at pH 5.5, which is the pH of the vacuoles), whereas citrate and oxalate could not. However, the malate concentration is not linearly correlated to Zn (Fig. 2). These results differ from those obtained by Zhao *et al*. (2000) on *A. halleri* plants grown in hydroponics, in which malate and citrate were correlated to Zn in the roots, but not in the aerial parts.

Zn Speciation in the bulk samples

The Zn K-edge EXAFS spectra for all plant samples are shown in Fig. 3. The whole set of data was first treated by principal component analysis (PCA) (Ressler *et al.*, 2000 and references therein). This statistical analysis allows the determination of the number of independent components contained in a set of spectra. The number of primary components corresponds to the number of Zn species present in the set of spectra, provided no species has a constant fractional amount (‘background’ species, Manceau et al., 2002). Then, an operation called "target transform" evaluates whether a reference spectrum is a likely principal component of the system. Once all components have been identified, their proportion in the various samples is determined by least-squares fitting of the unknown spectra to the combination of reference spectra previously identified by PCA. This approach is particularly powerful for the analysis of natural samples containing multiple forms of the same metal because the number and nature of these forms cannot be assumed *a priori* (Isaure et al., 2002). An important condition for the PCA is that the number of spectra should be greater than the number of unknown species, a condition amply satisfied here.

The number of primary components was evaluated from three criteria: the weight of each component, which is directly related to how much of the signal it represents, the indicator (IND) of each component, which reaches a minimum for the least significant component representing

real signal (Malinowski, 1991), and the residuals between experimental and reconstructed spectra using one, two, three, or more components. If the system contains two principal components, each spectrum should be well fitted by two components, and adding a third one should not significantly improve the quality of the fit.

In the present study, the weights of the first four components were, in decreasing order, 107, 44, 8, and 6, with IND values of 0.11, 0.04, 0.05 and 0.06, respectively. The spectra were correctly reconstructed with two components, with the normalized sum-square ($NSS = \Sigma[k^3 \chi(k)_{exp} - k^3 \chi(k)_{reconstr.}]^2 / \Sigma [k^3 \chi(k)_{exp}]^2$) between 3.7 x 10^{-2} and 4.2 x 10^{-3}, and the quality of the fits was not much improved with three components (*NSS* between 2.5 x 10^{-2} and 3.5 x 10^{-3}). Thus, it was concluded from this analysis that two Zn species are significantly present in the set of samples. Note that species representing less than 10% of total Zn are not detected by this method.

The two statistically-significant Zn species were subsequently identified by target transformation using a large library of reference spectra (aqueous Zn^{2+}, Zn complexed to organic acids, to amino acids, Zn sorbed on mineral surfaces, Zn minerals, Sarret *et al*, 1998a, Manceau *et al*., 2000). Several references gave satisfactory fits, including Zn malate, Zn histidine, aqueous Zn^{2+}, Zn citrate and Zn phytate. Other references, for instance Zn phosphate tetrahydrate or Zn oxalate gave unsatisfactory fits. Among the five compounds retained, the most likely pair of primary components should allow the reproduction of all the plant spectra by linear combinations of these two spectra. Thus, all possible pairs were tested, and Zn malate + Zn phytate was the only one satisfying this condition. Phytate, a *myo*-inositol *kis*-hexaphosphate, contains six phosphate groups, which lend the molecule a high affinity for cations (Cosgrove, 1980). In Zn phytate, the metal is four-fold coordinated (R = 1.96 Å), with a second shell modeled by only one

P atom at 3.08 Å, which corresponds to a disordered Zn phosphate environment. It is difficult to conclude on the presence of Zn phytate or disordered Zn phosphate mineral in the plant samples, so in the following text and in Table II, the generic term "Zn phosphate" will be used for this species. In this case study, the identification of the two species was facilitated by the fact that some samples were pure end-members, *i.e.*, contained 100% Zn malate or 100% Zn phosphate (Table II).

The percentage of Zn malate and Zn phosphate in each sample was estimated next by least-squares fitting the unknown spectra with linear combinations of the two references (Table II; Fig. 3 and 4). The fits pointed Zn malate as the major species in the aerial parts of the two *A. halleri* populations and in the roots of *A. halleri* from the contaminated soil. These results are consistent with malate/Zn ratios (higher than 1) except for the roots of *A. halleri* grown on soil (Table II). In this latter sample, citrate is well represented (138 $\mu mol\, g^{-1}$). The simulation of the EXAFS spectrum by a mixture of Zn malate (29 ± 10%), Zn citrate (39 ± 10%) and Zn phytate (32 ± 10%) gave a satisfactory fit, with a *NSS* of 5.3×10^{-2}. As Zn citrate was among the compounds positively identified by the target transformation, its presence in this sample is likely. The occurrence of Zn citrate in the other samples was tested by including Zn citrate as a third component of the simulations, but the proportions determined were always below 5 %, which is within the precision of the method. The fact that the PCA pointed out two instead of three principal components may be due to the fact that Zn citrate is present in only one sample, in which it represents less than 50% of total Zn.

The leaves of *A. h.* -C exposed to 10 µM Zn contained Zn malate plus a minor proportion (33 ± 10% of total Zn, *i.e.*, 4 $\mu mol\, g^{-1}$) of Zn phosphate. The fact that this Zn species was undetected at higher Zn concentration indicates that its proportion decreases when Zn increases (Fig. 4A). Zn

phosphate was clearly the major Zn species in the roots of all plants grown in hydroponics, and in the aerial parts of *A. lyrata* ssp. *petraea*.

Zn structural parameters determined by numerical fits confirmed the results obtained by PCA and linear combinations (Table III; Fig. 5). In the aerial parts of all *A. halleri* plants, Zn was found to be octahedrally coordinated (d(Zn-O) = 1.99 to 2.03 Å) and surrounded by a next-nearest C shell at 2.80 to 2.87 Å, in agreement with a Zn malate complex (Table III). In the roots of the hydroponic plants, and in the aerial parts of *A. lyrata* ssp. *petraea*, the Zn-O distance (d(Zn-O) = 1.95 to 1.99 Å) is characteristic of a tetrahedral coordination, and the next-nearest shell consists of P atoms at 3.06 to 3.16 Å as in phosphate compounds. Samples containing several Zn species (roots of *A. h.* -C grown on soil and aerial parts of *A. h.* -C grown in the 10 µM solution), have Zn structural parameters intermediate between those of the two (Zn malate and Zn phytate) or three (Zn malate, Zn citrate and Zn phytate) references.

Zn Speciation in the trichomes of *A. halleri*

High Zn concentrations were recently observed in the bases of the trichomes in the leaves of *A. halleri* (Küpper *et al.*, 2000, Zhao *et al.*, 2000). The distribution and speciation of Zn in the leaves of *A. h.* -C grown on the contaminated soil were investigated at the micron scale using µSXRF and Zn K-edge µEXAFS spectroscopy. Elemental maps of Ca and various metals present in the leaves are presented in Fig. 6. Ca is almost evenly distributed in the leaf, whereas transition metals are concentrated in the bases of the trichomes. For instance, Zn signal is about 10-fold greater in these spots than in the leaf itself (75000 cts/s/I_0 compared to 4000-8000 cts/s/I_0). Considering the thickness of the leaf and of the trichome spots, it corresponds to a Zn concentration at least 100-fold higher. The same elemental distribution was observed in other leaves of different ages. Zn-K-edge µEXAFS spectra in different Zn ‘hot spots’ were recorded

and found to be identical. Figure 7 compares the μEXAFS spectrum of a trichome to the EXAFS spectra of the roots and aerial parts of *A. h.* -C, together with a selection of Zn references. The trichome spectrum is clearly different from all the others: Its frequency matches that of the roots of *A. h.* -C grown in hydroponics, but the two spectra clearly have a distinct shape. The trichome spectrum was compared to a large number of Zn organic and mineral references (see previous paragraph), but no good match was obtained. The occurrence of mineral Zn in this highly metal-concentrated zone was ruled out, as EXAFS spectra of inorganic compounds such as zincite or hydrozincite exhibit complex shapes owing to the presence of heavy atoms in the second or higher coordination shells (Fig. 7). The comparison of the radial distribution function (RDF) for the trichome and the bulk plant samples indicates that Zn is tetrahedrally coordinated, as in the roots of the hydroponic plant (Fig. 8). The second shell peak of the trichome is centered at $R + \Delta R = 2.5$ Å, compared to 2.6 Å for the aerial parts (C shell) and 2.8 Å for the roots (P shell). This short distance is suggestive of a C shell (Sarret *et al.*, 1998a). This structural interpretation is strongly supported by the relative position of the modulus and imaginary part of the Fourier transform, whose maxima are superimposed in the case of a Zn-P pair, and opposite for a Zn-C pairs (see arrows in Fig. 8, and Sarret *et al.*, 1998a). Hence, the second coordination shell of Zn in the trichome likely consists of C atoms.

These data suggest that in the bases of the trichomes, Zn is four-fold coordinated and complexed to carboxyl and/or hydroxyl groups belonging to organic acid(s). This chemical form differs from the average form (*i.e.*, Zn malate) identified by powder EXAFS, which means that it is quantitatively minor. Despite the high concentration of Zn in the base of the trichomes, these cells account for a minor proportion of the leaf biomass, so they do not represent the major sink of Zn. The combination of μEXAFS and powder EXAFS shows that the metal is distributed as

Zn malate in the leaf itself (predominant form), and as a tetrahedral Zn-organic acid(s) complex in the trichomes (minor form).

DISCUSSION

A. halleri is supposed to accumulate Zn in the vacuolar compartment of the leaves (Neumann & zur-Nieden, 2001), similarly to *T. caerulescens* (Frey *et al.*, 2000, Küpper *et al.*, 1999, Vazquez *et al.*, 1992). Organic acids, including malate, citrate, and oxalate, which are primarily located in the vacuoles (Ryan & Walker-Simmons, 1983), thus are often inferred to chelate metals. In *Thlaspi caerulescens*, malate was shown to be the most abundant organic acid in the shoots (164 to 248 µmol g^{-1} f. w.), followed by citrate, succinate and oxalate (Tolra *et al.*, 1996). However, XANES spectroscopy showed that malate was not involved in Zn binding in this species, the chemical forms of Zn being, in decreasing proportion, citrate, aqueous Zn^{2+}, histidine, and Zn bound to the cell wall (Salt *et al.*, 1999). In the present study, EXAFS and chemical analyses showed that Zn is predominantly complexed to malate in the leaves of the two *A. halleri* populations. A secondary Zn organic species was identified in the trichomes, in which Zn is tetrahedrally coordinated and complexed to carboxyl and/or hydroxyl functional groups. The function of the trichomes in metal storage or exudation is still unclear.

Although *A. lyrata* ssp. *petraea* has a malate/Zn molar ratio much higher than 1 in its aerial parts, this non-tolerant and non-hyperaccumulating species sequesters Zn as a phosphate species, similarly to various crop species (van Steveninck *et al.*, 1994, Sarret *et al.*, 2001). The fact that malate is not a marker of tolerance and hyperaccumulation is also supported by Shen *et al.*'s results (1997), who showed that the hyperaccumulator *T. caerulescens* and the non-tolerant and non-hyperaccumulator *T. ochroleucum* had constitutively high concentrations of malate in shoots. Instead, the location of malate (vacuolar or cytoplasmic) and the quantity of Zn transmembrane

transporters (Lasat *et al.*, 2000, Pence *et al.*, 2000, Assunçaõ *et al.*, 2001) are probably key factors conditioning Zn hyperaccumulation.

In the roots of hydroponic plants, Zn was speciated as inorganic or organic Zn phosphate. As phosphate precipitates have been observed previously at the root surface of hydroponic plants (Küpper *et al.*, 2000, Zhao *et al.*, 2000), the inorganic form is more likely. Although the nutrient solutions were undersaturated with respect to Zn-phosphate solids, chemical precipitation may have been induced by the root activity. This phenomenon would account for the low measured values of the root-to-leaf transfer coefficients (Table I). Zn phosphate was also present in small proportion in the roots of the plant grown on soil. Its location, either at the surface of the roots or inside the cells, is unknown, but the high phosphorus content of the soil (3 to 4 g kg^{-1} d. w. P_2O_5) tends to favor the first hypothesis.

These results were obtained on freeze-dried and ground plant materials for bulk EXAFS experiments, and on freeze-dried whole leaves for µEXAFS experiments. For bulk EXAFS, grinding is required to obtain homogeneous samples at the scale of the X-ray beam (a few hundreds of micrometers in our experiment). To avoid chemical reactions between different cell compartments during this step, the plant material can be frozen or freeze-dried. This latter conditioning was preferred in order to avoid a possible partial defrosting and mixing of the cell compartments during grinding or sample transfer. However, it is difficult to completely dismiss the possibility of artifacts induced by this preparation. For instance, could Zn malate and Zn phosphate be the products of reactions occurring during the dehydration between Zn^{2+}, malate and phosphate ions ? The high affinity of Zn^{2+} for malate and phosphate (complexation constant log K = 2.9 for Zn malate (Smith & Martell, 1982)), solubility constant log K_S = –32 for Zn phosphate tetrahydrate (MINTEQA2 database)) is a point in favor of the preexistence of the two species in the fresh material. Moreover, these reactions would imply proton exchange, whose

possible occurrence at low temperature (-52°C in the freeze-dryer used in this work) is unknown to our knowledge.

In conclusion, the major, and some minor, chemical forms of Zn in the aerial parts and in the roots of *A. halleri* and *A. lyrata* ssp. *petraea* have been elucidated at the molecular-scale by the combination of chemical analyses and EXAFS spectroscopy. However, the role of the genes involved in Zn tolerance and hyperaccumulation on the speciation of Zn is still unknown. In addition, the biochemical processes responsible for Zn absorption, transfer, and storage remain to be clearly delineated.

MATERIALS AND METHODS

Plant origins

Seeds of *A. halleri* were collected on single mother plants in 1999 at two different sites. Seeds of *A. halleri* from the polluted site (*A. h.*-C) were collected in a field contaminated by the atmospheric fallouts of a nearby Zn smelter in Auby (North of France). Seeds of *A. halleri* of non-contaminated origin (*A. h.* -NC) were collected in Tatransla Javorina, a conservation area of the High Tatras in Slovakia. *A. lyrata* ssp. *petraea* (*A. l.*) originated from Unhošt, an uncontaminated woodland in the valley of Lodenice in Central Bohemia (Czech Republic).

Plant culture

Seeds were germinated on sand in a greenhouse, and eight weeks after germination seedlings were transferred to 10L polycarbonate vessels (6 plants per vessel) containing a growth medium. The medium consisted of 0.5 mM $Ca(NO_3)_2$, 0.2 mM $MgSO_4$, 0.5 mM KNO_3, 0.1 mM K_2HPO_4, 0.2 µM $CuSO_4$, 2 µM $MnCl_2$, 10 µM H_3BO_3, 0.1 µM MoO_3, 10 µM FeEDDHA, and 0.2 µM

$ZnSO_4$. The vessels were kept in a controlled-growth chamber (temperature 20°C day / 15°C night; light 16h day / 8h night). The pH of the solution was maintained at 5.0 ± 0.1 using 2-morpholinoethanesulphonic (MES) acid buffer (2 mM), which is known to be chemically inert towards metals. After three weeks, the nutrient solutions received $ZnSO_4$ at the following concentrations: 10, 100 or 250 μM for *A. h.*-C, 100 or 250 μM for *A. h.*-NC (the plants grown on 10 μM were accidentally lost), and 10 μM for *A. l.* (1 vessel containing 6 plants per Zn concentration). The theoretical speciation of Zn in the nutrient solutions was calculated using MINTEQA2 program. Zn speciation was almost constant at the three Zn concentration, with free Zn^{2+} as major species (84 to 85 %), and aqueous $ZnSO_4$ as minor species (15 to 16 %). The saturation indexes for Zn minerals were always negative, so no Zn precipitates should have formed. During the experiment, nutrient solutions were renewed every 8 days. The position under lights in the growth chamber was randomly modified each 4 days. Plants were harvested after 5 weeks of Zn treatment. In parallel to the hydroponic culture, six *A. halleri* plants growing naturally in the polluted site of Auby were sampled. After harvesting, plant samples were rinsed with deionized water and divided into roots and aerial parts. For each species and each culture condition, the roots and the aerial parts of the six plants were pooled in order to have enough material for the EXAFS and chemical analyses and freeze-dried. To allow a rapid freezing, each sample was placed in a large container, transferred into the freeze-dryer at room temperature, and the container was filled with liquid nitrogen before starting the dehydration. The samples were then ground using a mechanical agate mill. An aliquot was kept for EXAFS, and the rest was divided into six aliquots, three for the analysis of Zn and P, and three for the analysis of organic acids. Some freeze-dried leaves of *A. halleri* from the contaminated site were kept for μSXRF and μEXAFS analysis.

Chemical Analyses

For Zn and P analysis, plant powders were digested with $HNO_3/HClO_4$ (80:20, v/v) and Zn and P concentrations were determined using inductively coupled atomic emission spectrometry (ICP-AES). For the determination of malic, citric and oxalic acid concentrations, the plant powders were placed in a 0.1 N HCl solution and ultrasonicated for 1 hour in order to extract and dissociate the Zn-organic acids complexes. The suspension was then filtered at 0.45 µm, and cations were extracted from the solution using a cationic exchange resin (On Guard H Dionex). The solution was then neutralized to pH 7 using a 1 N NaOH solution. Organic acids concentrations were measured by ionic chromatography (Dionex DX500). All values are given as mean concentrations over three samples ± standard deviation.

X-ray Absorption Spectroscopy

Zn malate standard was obtained by slow evaporation of a solution containing 10^{-2} M $Zn(NO_3)_2$ and 8 10^{-2} M Na malate at pH 5.5. Zn citrate was purchased from Alfa. Zn phytate was kindly provided by J. Cotter-Howells. Other Zn standards were presented previously (Sarret *et al.*, 1998a, b, Manceau *et al.*, 2000, Isaure *et al.*, 2002). Pressed pellets were prepared from the aerial parts and roots powder. Zn K-edge EXAFS spectra of Zn-rich samples were measured at room temperature on beamline D42 at the Laboratoire du Rayonnement Electromagnétique (LURE, Orsay, France) in transmission mode using ionization chambers, and on beamline BM32 at the European Synchrotron Radiation Facility (ESRF, Grenoble, France) in fluorescence mode using a 30-element solid-state Ge detector (Canberra) for diluted samples ([Zn] < 5000 mg kg^{-1}). Data extraction was performed according to standard methods. The principal component analysis

and the least-squares spectral decomposition were performed with our own software, and EXAFS structural parameters (coordination numbers, interatomic distances, and Debye Waller factors) were determined using WinXAS 2.0 (Ressler, 1997). For this determination, k^3-weighted $\chi(k)$ functions were Fourier transformed over the 3.5-12 $Å^{-1}$ range using a Bessel window with a smoothing parameter of 4. Then fits of the first two shells were carried out using Zn-O, Zn-P and Zn-C theoretical scattering functions calculated with FEFF7 (Rehr *et al*., 1991) from the structure of Zn malate dihydrate (Reed & Karipides, 1976) and hopeite (Whitaker, 1975). Fits were performed both in *k* and *R* space to check for consistency.

Microprobe analyses

µSXRF and Zn K-edge µEXAFS measurements on the leaves of *A. h*.-C grown on the soil were performed on beamline 10.3.2 at the Advanced Light Source (ALS, Berkeley, USA), operating at 1.9 GeV and 200-400 mA. Fragments of freeze-dried leaves were fixed on a kapton tape, mounted on a x-y translation stage, and studied in air at room temperature. The beam was focused using a pair of elliptically bent mirrors in the Kirkpatrick-Baez configuration (Kirkpatrick & Baez, 1948). The incident beam intensity was measured using two copper paddles forming a miniature ionization chamber, and the fluorescence yield was measured using a seven-element Ge solid-state detector. For µSXRF, the spot size was 5*5 µm, and the fluorescence yield was normalized by I0 and the dwell time. Four maps of different leaves were recorded. For µEXAFS, the spot size was 15*5 µm. Three µEXAFS scans were performed on a Zn-rich trichome from three different leaves. All spectra were identical.

ACKNOWLEDGMENTS

We would like to acknowledge the European Synchrotron Radiation Facility (ESRF) in Grenoble, the LURE in Orsay, and the Advanced Light Source (ALS) in Berkeley for the provision of beamtime. We are grateful to Vlastimil Mikolas for help in finding population sites in Slovakia, to Marc Macnair for providing seeds of *Arabidopsis lyrata* ssp. *petraea*, to Nicolas Geoffroy for his technical support, and to Jaco Vangronsveld for fruitful discussions.

LITERATURE CITED

Assunçaõ AGL, Martins PD, De Folter S, Vooijs R, Schat H, Aarts MGM (2001) Elevated expression of metal transporter genes in three accessions of the metal hyperaccumulator *Thlaspi caerulescens*. Plant Cell and Environment **24**: 217-226

Baker AJM, Walker PL (1990) Ecophysiology of metal uptake by tolerant plants. In AJ Shaw, ed. Heavy Metal Tolerance in Plants: Evolutionary Aspects. CRC Press, Boca Raton, pp 155-177

Baker AJM, McGrath SP, Reeves RD, Smith JAC (2000) Metal hyperaccumulator plants: a review of the ecology and physiology of a biochemical resource for phytoremediation of metal-polluted soils. In N Terry, G Banuelos, J Vangronsveld, eds. Phytoremediation of Contaminated Soil and Water. Lewis Publishers, Boca-Raton, pp 85-107

Bert V, Macnair MR, De Laguerie P, Saumitou-Laprade P, Petit D (2000) Zinc tolerance and accumulation in metallicolous populations of *Arabidopsis halleri* (Brassicaceae). New Phytol **146**: 225-233

Bert V, Bonnin I, Saumitou-Laprade P, de Laguérie P, Petit D (2002) Heavy metal (Zn, Cd, Pb) accumulation in natural populations of *Arabidopsis halleri* from contaminated and normal habitats, New Phytol, in press

Brooks RR (1998) Plants That Hyperaccumulate Heavy Metals. CAB International, Wallingford.

Chao GY (1969) Refinement of the crystal structure of parahopeite. Zeits Krist **130**: 261-266

Cosgrove DJ (1980) Inositol Phosphate. Their Chemistry, Biochemistry and Physiology. Elsevier, New York.

Dahmani-Muller H, Van-Oort F, Gelie B, Balabane M (2000) Strategies of heavy metal uptake by three plant species growing near a metal smelter. Environ Pollut **109**: 231-238

Epstein E (1999) Silicon. Annual review of Plant Physiology. Plant Mol Biol **50**: 641-664

Frey B, Keller C, Zierold K, Schulin R (2000) Distribution of Zn in functionally different leaf epidermal cells of the hyperaccumulator *Thlaspi caerulescens*. Plant Cell and Environ **23**: 675-687

Isaure MP, Laboudigue A, Manceau A, Sarret G, Tiffreau C, Trocellier P, Lamble G, Hazemann JL, Chateigner D (2002) Quantitative Zn speciation in a contaminated dredged sediment by µ-PIXE, µ-SXRF, EXAFS spectroscopy and principal component analysis. Geochim Cosmochim Acta **66**: 1549-1567

Kaul S, et al. (2000) Analysis of the genome sequence of the flowering plant *Arabidopsis thaliana*. Nature **408**: 796-815

Kirkpatrick P & Baez AV (1948) Formation of optical images by X-rays. J Opt Soc Am **38:** 766

Koch M, Haubold B, Mitchell-Olds T (2001) Molecular systematics of the Brassicaceae: evidence from coding, plastidic *MatK* and nuclear *Chs* sequences. Am J Botany **88**: 534-544

Küpper H, Lombi E, Zhao FJ, McGrath SP (2000) Cellular compartmentation of cadmium and zinc in relation to other elements in the hyperaccumulator *Arabidopsis halleri*. Planta **212**: 75-84

Küpper H, Zhao FJ, McGrath SP (1999) Cellular compartmentation of zinc in leaves of the hyperaccumulator *Thlaspi caerulescens*. Plant Physiol **119**: 305-311

Lasat, M.M., Pence NS, Garvin DF, Ebbs SD, Kochian LV (2000) Molecular physiology of zinc transport in the Zn hyperaccumulator *Thlaspi caerulescens*. J Exp Botany **51**: 71-79

Lasat MM, Baker AJM, Kochian LV (1998) Altered Zn compartmentation in the root symplasm and stimulated Zn absorption into the leaf as mechanisms involved in Zn hyperaccumulation in *Thlaspi caerulescens*. Plant Physiol **118**: 875-883

Macnair MR, Baker AJM (1994) Metal tolerance in plants: Evolutionary aspects. In M E Farago, ed. Plants and the Chemical Elements. VCH, Weinheim, Germany, pp 68-86

Macnair MR, Bert V, Huitson SB, Saumitou-Laprade P, Petit D (1999) Zinc tolerance and hyperaccumulation are genetically independent characters. Proceedings of the Royal Society of London **B 266**: 2175-2179

Malinowski ER (1991) Factor Analysis in Chemistry. John Wiley, New York.

Manceau A, Lanson B, Schlegel ML, Hargé JC, Musso M, Eybert-Bérard L, Hazemann JL, Chateigner D, Lamble GM (2000) Quantitative Zn speciation in smelter-contaminated soils by EXAFS spectroscopy. Am J Sci **300**: 289-343

Manceau A, Marcus MA, and Tamura N (2002) Quantitative speciation of heavy metals in soils and sediments by synchrotron X-ray techniques. In N.C. Sturchio, P. Fenter, S.R. Sutton, M.L. Rivers, eds. Applications of Synchrotron Radiation in Low-Temperature Geochemistry and Environmental Science. Reviews in Mineralogy, Mineralogical Society of America, Washington D.C., in press

Meinke DW, Cherry JM, Dean C, Rounsley SD, Koornneef M (1998) *Arabidopsis thaliana*: A model plant for genome analysis. Science **282**: 662

Neumann D, zur-Nieden U (2001) Silicon and heavy metal tolerance of higher plants. Phytochem **56**: 685-692

Nriagu JO, Pacyna JM (1988) Quantitative assessment of worldwide contamination of air, water and soils by trace metals. Nature **333**: 134-139

Pence NS, Larsen PB, Ebbs SD, Letham DLD, Lasat MM, Garvin DF, Eide D, Kochian LV (2000) The molecular physiology of heavy metal transport in the Zn/Cd hyperaccumulator *Thlaspi caerulescens*. Proceedings of the National Academy of Sciences of the United States of America **97**: 4956-4960

Pollard AJ, Baker AJM (1996) The quantitative genetics of zinc hyperaccumulation in *Thlaspi caerulescens*. New Phytol **132**: 113-118

Reed AT, Karipides A (1976) The crystal structure of S-Malatodiaquozinc(II) hydrate. Acta Cryst **B32**: 2085

Rehr JJ, Mustre de Leon J, Zabinsky SI, Albers RC (1991) Theoretical X-ray absorption fine structure standards. J Am Chem Soc **113**: 5135-5145

Ressler T (1997) WinXAS: A new software package not only for the analysis of energy-dispersive XAS data. J Physique IV **7**: c2-269

Ressler T, Wong J, Roos J, Smith IL (2000) Quantitative speciation of Mn-bearing particulates emitted from autos burning (methylcyclopentadienyl)manganese tricarbonyl-added gasolines using XANES spectroscopy. Environ Sci Technol **34**: 950-958

Rodriguez E, Healey PL, Mehta I (1983) Biology and Chemistry of Plant Trichomes. Plenum Press, New-York

Ryan CA, Walker-Simmons M (1983) Plant vacuoles. Methods Enzymol **96**: 580-589

Salt DE, Prince RC, Baker AM, Raskin I, Pickering IJ (1999) Zinc ligands in the metal hyperaccumulator *Thlaspi caerulescens* as determined using X-ray absorption absorption spectroscopy. Environ Sci Technol **33**: 713-717

Sarret G, Manceau A, Spadini L, Roux JC, Hazemann JL, Soldo Y, Eybert-Bérard L, Menthonnex JJ (1998a) Structural determination of Zn and Pb binding sites in *Penicillium chrysogenum* cell walls by EXAFS spectroscopy. Environ Sci Technol **32**: 1648-1655

Sarret G, Manceau A, Cuny D, Van Haluwyn C, Deruelle S, Hazemann JL, Soldo Y, Eybert-Bérard L, Menthonnex JJ (1998b) Mechanism of lichen resistance to metallic pollution. Environ Sci Technol **32**: 3325-3330

Sarret G, Vangronsveld J, Manceau A, Musso M, D'Haen J, Menthonnex JJ, Hazemann JL (2001) Accumulation forms of Zn and Pb in *Phaseolus vulgaris* in the presence and absence of EDTA. Environ Sci Technol **35**: 2854 -2859

Shen ZG, Zhao FJ, McGrath SP (1997) Uptake and transport of zinc in the hyperaccumulator *Thlaspi caerulescens* and the non-hyperaccumulator *Thlaspi ochroleucum*. Plant Cell Environ **20**: 898-906

Smith RM & Martell AE (1982) Critical Stability Constants, Vol 3. Plenum Press, New-York, pp 126

Streit B & Stumm W (1993) Chemical Properties of Metals and the Process of Bioaccumulation in Terrestrial Plants. In B. Markert, ed. Plants as Biomonitors. VCH, Weinheim, Germany, pp 29-62

Tolra RP, Poschenrieder C, Barcelo J (1996) Zinc hyperaccumulation in *Thlaspi caerulescens*. II. Influence on organic acids. J Plant Nutr **19**: 1541-1550

Van Der Lelie N, Schwitzguebel JP, Glass DJ, Vangronsveld J, Baker A (2001) Assessing phytoremediation's progress in the United States and Europe. Environ Sci Technol **35**: 446 A–452 A

Van Steveninck RFM, Barbare A, Fernando DR, Van Steveninck ME (1994) The binding of zinc, but not cadmium, by phytic acid in roots of crop plants. Plant and Soil **167**: 157-164

Vazquez MD, Barcelo J, Poschenrieder C, Madico J, Hatton P, Baker AJM, Cope GH (1992) Localization of zinc and cadmium in *Thlaspi caerulescens* (brassicaceae), a metallophyte that can hyperaccumulate both metals. J Plant Physiol **140**: 350-355

Vazquez MD, Poschenrieder C, Barcelo J, Baker AJM, Hatton P, Cope GH (1994) Compartmentation of zinc in roots and leaves of the zinc hyperaccumulator *Thlaspi caerulescens* J & C Prel. Bot Acta **107**: 243-250

Verkleij JAC & Schat H (1989) Mechanisms of metal tolerance in higher plants. In A.J. Shaw, ed. Heavy Metal Tolerance in Plants: Evolutionary Aspects. CRC Press, Boca Raton, pp 179-193

Whitaker A (1975) The crystal structure of hopeite, $Zn_3(PO_4)_2$, $4H_2O$. Acta Cryst **B31**: 2026-2035

Zhao FJ, Lombi E, Breedon T, McGrath SP (2000) Zinc hyperaccumulation and cellular distribution in *Arabidopsis halleri*. Plant Cell Environ **23**: 507-514.

Table I. *Zn, P, malate, citrate and oxalate concentrations in the roots (R) and in the aerial parts (AP) of the plants.*

		Concentrations ($\mu mol\ g^{-1}$)											
		Zn			P		Malate		Oxalate		Citrate	
Plants Grown in Hydroponics	*[Zn] solution* (μM)	*R*	*AP*	*T* [a]	*R*	*AP*	*R*	*AP*	*R*	*AP*	*R*	*AP*
A. h. –C	250	218 ± 15	160 ± 1	0.7	469 ± 5	67 ± 2	2 ± 1	165 ± 24	5 ± 0	5 ± 0	22 ± 4	31 ± 5
	100	105 ± 15	62 ± 1	0.6	419 ± 57	74 ± 6	6 ± 1	144 ± 28	5 ± 0	16 ± 3	10 ± 1	19 ± 5
	10	17 ± 4	11 ± 2	0.6	181 ± 45	67 ± 12	6 ± 0	113 ± 6	4 ± 0	18 ± 9	28 ± 7	18 ± 1
A. h. –NC	250	218 ± 30	217 ± 19	1.0	551 ± 54	73 ± 7	5 ± 2	221 ± 35	5 ± 0	10 ± 3	9 ± 1	6 ± 0
	100	74 ± 13	80 ± 3	1.1	239 ± 47	56 ± 7	21 ± 6	111 ± 32	5 ± 1	8 ± 4	56 ± 10	16 ± 5
A. l.	10	46 ± 2	6 ± 0	0.1	292 ± 2	77 ± 3	10 ± 4	220 ± 22	0 ± 0	0 ± 0	9 ± 1	10 ± 1
Plant from the Contaminated Soil												
A. h. –C	–	112 ± 11	169 ± 8	1.5	70 ± 5	95 ± 2	36 ± 5	447 ± 26	6 ± 0	34 ± 7	138 ± 24	59 ± 6

Values are means of three samples ± SD. *A. h.* -C, *Arabidopsis halleri*, contaminated origin; *A. h*. -NC, *Arabidopsis halleri*, non-contaminated origin; *A. l.*, *Arabidopsis lyrata* ssp. *petraea*. [a] Transfer coefficient = $[Zn]_{aerial\ parts}/[Zn]_{roots}$.

Table II. *Proportion and amount of Zn malate and Zn phosphate species in the plant samples.*

			EXAFS					Chemical Analyses	
	$[Zn]_{sol.}$ (μM)	*[Zn]* ($\mu mol\ g^{-1}$)	Proportion of Zn Species [a] (molar % of total Zn)			Concentrations [b] ($\mu mol\ g^{-1}$)		Concentrations ($\mu mol\ g^{-1}$)	
Aerial parts			Zn Malate	Zn Phosphate	*NSS* $x10^{-2}$ [c]	Zn Malate	Zn Phosphate	Malate	P
A. h. –C	250	160 ± 1	100 ± 10	0 ± 10	2.5	160 ±17	0 ± 16	165 ± 24	67 ± 2
	100	62 ± 1	100 ± 10	0 ± 10	4.1	62 ± 7	0 ± 6	144 ± 28	74 ± 6
	10	11 ± 2	67 ± 10	33 ± 10	5.6	7 ± 3	4 ± 2	113 ± 6	67 ± 12
A. h. –NC	250	217 ± 19	100 ± 10	0 ± 10	5.9	217 ± 43	0 ± 24	221 ± 35	73 ± 7
	100	80 ± 3	100 ± 10	0 ± 10	3.3	80 ± 11	0 ± 8	111 ± 32	56 ± 7
A. l.	10	6 ± 0	0 ± 10	100 ± 10	13.4	0 ± 1	6 ± 1	220 ± 22	77 ± 3
A. h. -C (soil)	–	169 ± 8	100 ± 10	0 ± 10	3.9	169 ± 26	0 ± 18	447 ± 26	95 ± 2
Roots									
A. h. –C	250	218 ± 15	0 ± 10	100 ± 10	9.4	0 ± 23	218 ± 38	2 ± 1	469 ± 5
	100	105 ± 15	0 ± 10	100 ± 10	14.8	0 ± 12	105 ± 27	6 ± 1	419 ± 57
	10	17 ± 4	0 ± 10	100 ± 10	9.4	0 ± 2	17 ± 6	6 ± 0	181 ± 45
A. h. –NC	250	218 ± 30	0 ± 10	100 ± 10	7.4	0 ± 25	218 ± 55	5 ± 2	551 ± 54
	100	74 ± 13	0 ± 10	100 ± 10	10.9	0 ± 9	74 ± 22	21 ± 6	239 ± 47
A. l.	10	46 ± 2	0 ± 10	100 ± 10	10.3	0 ± 5	46 ± 7	10 ± 4	292 ± 2
A. h. -C (soil) [d]	–	112 ± 11	75 ± 10	25 ± 10	3.6	84 ± 21	28 ± 15	36 ± 5	70 ± 5
			Zn Malate	Zn Citrate	Zn Phosphate	Zn Malate	Zn Citrate	Zn Phosphate	Malate	Citrate	P
			29 ± 10	39 ± 10	32 ± 10	5.3	33 ± 15	44	35 ± 16	36 ± 5	138 ± 24	70 ± 5

A. h. -C, *Arabidopsis halleri*, contaminated origin; *A. h.* -NC, *Arabidopsis halleri*, non-contaminated origin; *A. l.*, *Arabidopsis lyrata* ssp. *petraea*. [a] Proportions of Zn species (in molar % of total Zn) were determined by simulating the plant EXAFS spectra by a linear combination of Zn malate and Zn phytate spectra (Fig. 3). [b] Concentrations are calculated from the proportion of the two species and the total Zn concentrations (Table I). [c] The quality of the fit is estimated by the normalized sum-square $NSS = \Sigma[k^3\ \chi(k)_{exp} - k^3\ \chi(k)_{reconstr.}]^2 / \Sigma\ [k^3\ \chi(k)_{exp}]^2$). [d] For this sample, two Zn distributions are given', one including Zn malate and Zn phytate, and one including Zn citrate as well. The error bars correspond to an uncertainty of 10% for the proportion of Zn species, to the standard deviation over three samples for the measured concentrations, and to the combination of both uncertainties for the deduced concentrations of Zn species.

Table III. *Zn structural parameters in reference compounds and plant samples.*

		1st Shell (O)			2nd Shell				
		N	*R* (Å)	σ^2 (Å^2)	Atom	*N*	*R* (Å)	σ^2 (Å^2)	*Res*[a]
Reference Compounds									
Zn Phytate		3.9	1.96	0.008	P	1.0	3.08	0.010	16
Zn Malate		4.2	2.01	0.010	C	1.9	2.80	0.012	14
Zn Citrate		4.3	2.03	0.010	C	3.5	2.76	0.012	12
Plant Samples									
Aerial parts	$[Zn]_{solution}$ (μM)								
A. h. -C	250	4.5	2.01	0.010	C	1.9	2.87	0.009	16
	100	4.3	2.01	0.010	C	1.5	2.81	0.012	16
	10	3.7	1.99	0.009	C	2.0	2.86	0.010	24
A. h. -NC	250	4.5	2.03	0.010	C	2.1	2.80	0.012	17
	100	4.3	2.01	0.010	C	1.9	2.84	0.010	15
A. l.	10	4.1	1.99	0.010	P	1.3	3.07	0.011	17
A. h. –C (soil)	–	4.6	2.01	0.010	C	0.6	2.80	0.012	17
Roots									
A. h. -C	250	4.1	1.96	0.007	P	1.3	3.09	0.008	15
	100	4.3	1.95	0.007	P	1.5	3.09	0.009	15
	10	4.3	1.97	0.009					11
A. h. -NC	250	4.2	1.96	0.007	P	1.1	3.10	0.007	15
	100	4.0	1.96	0.008	P	1.7	3.16	0.009	8
A. l.	10	4.0	1.98	0.009	P	1.2	3.06	0.011	14
A. h. –C (soil)	–	4.3	2.00	0.011	C	1.2	2.77	0.012	18

Structural parameters were obtained by simulating the first two coordination shells of Zn. *A. h*. -C, *Arabidopsis halleri*, contaminated origin; *A. h*. -NC, *Arabidopsis halleri*, non-contaminated origin; *A. l*., *Arabidopsis lyrata* ssp. *petraea*. *N,* coordination number; *R,* interatomic distance (Å); σ^2, Debye-Waller disorder factor (Å^2). [a] The quality of the fit is estimated by the residual $Res = \Sigma \left| k^3 \chi(k)_{exp} - k^3 \chi(k)_{fit} \right| / \Sigma \left| k^3 \chi(k)_{exp} \right| * 100$. Estimated errors on *R* and *N* are $\pm$ 0.01 Å and $\pm$ 10% for the first shell, $\pm$ 0.03 Å and $\pm$ 20% for the second shell, respectively.

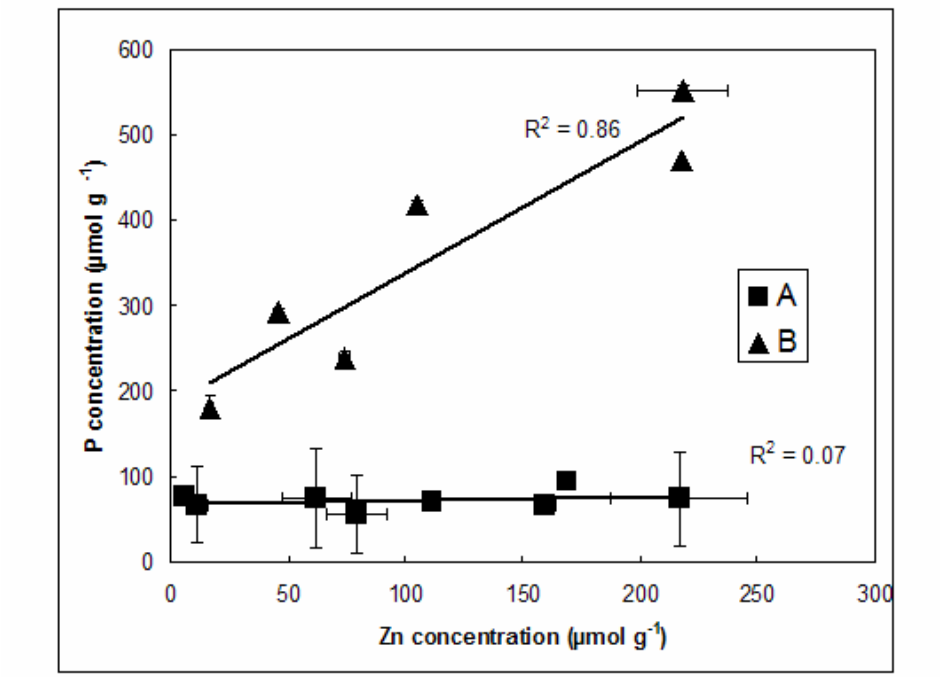

Figure 1. Relationship between Zn and P concentrations in the plant samples. Two groups of points can be defined: The first one (group A) represents the aerial parts of all plants and the roots of *A. halleri* from the contaminated soil. For these samples, Zn and P are not correlated (R2, regression coefficient = 0.07). The second group (group B) represents the roots of all plants, except those of *A. halleri* from the contaminated soil. A Zn-P correlation clearly exists for these samples (R2 = 0.86).

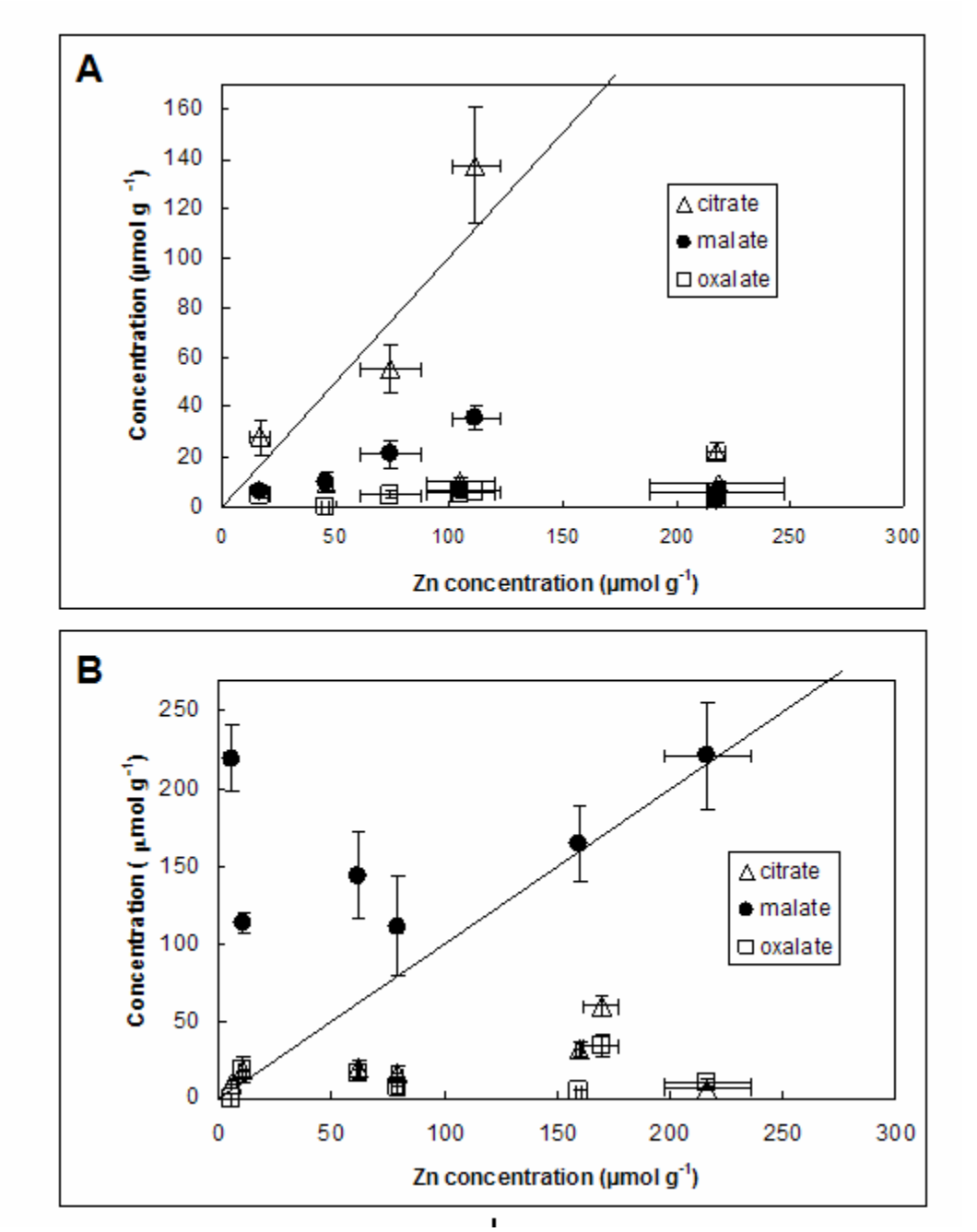

Figure 2. Organic acids content as a function of Zn content in the roots (A) and in the aerial parts (B) of the plants (values given in Table I). The line y = x is shown in each plot.

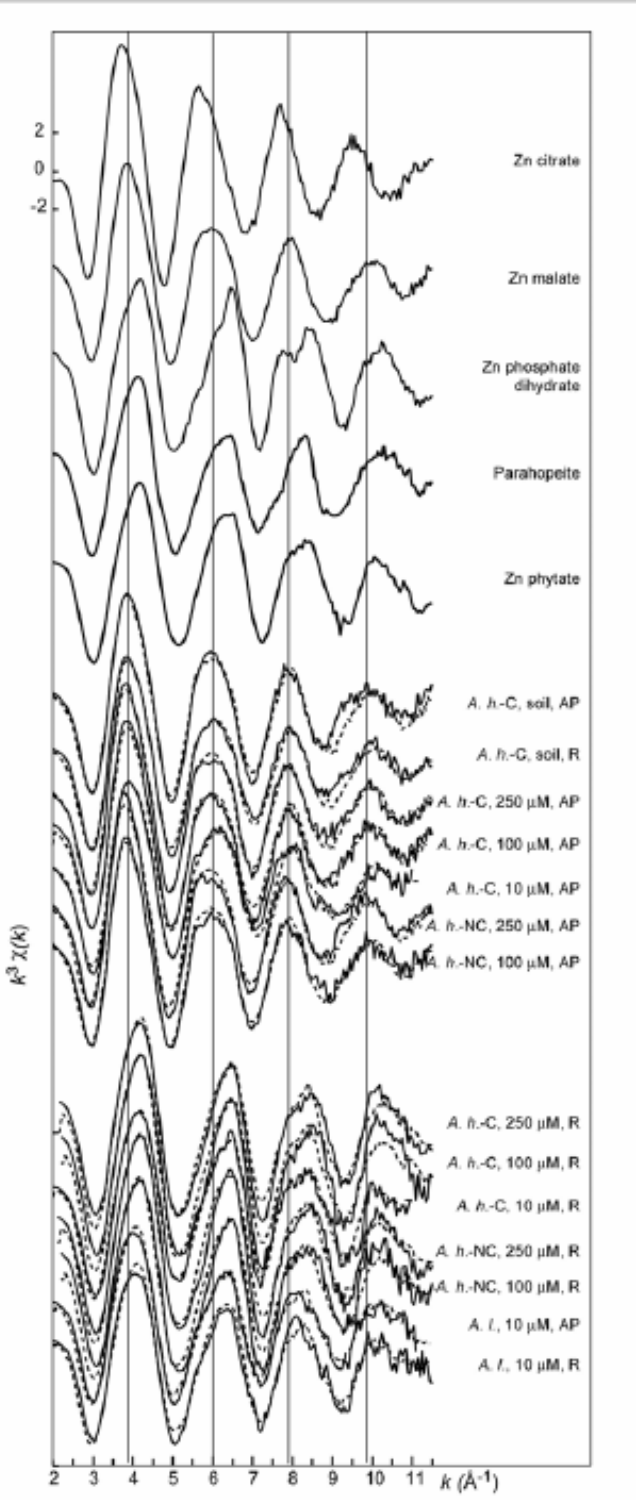

Figure 3. Zn K-edge EXAFS spectra for the plant samples (*A. h.* -C, *Arabidopsis halleri*, contaminated origin; *A. h*. -NC, *Arabidopsis halleri*, uncontaminated origin; *A. l*., *Arabidopsis lyrata* ssp. *petraea*; R, roots; AP, aerial parts) and for some Zn reference compounds. Solid lines are data and dashed lines are linear combinations of Zn malate and Zn phytate.

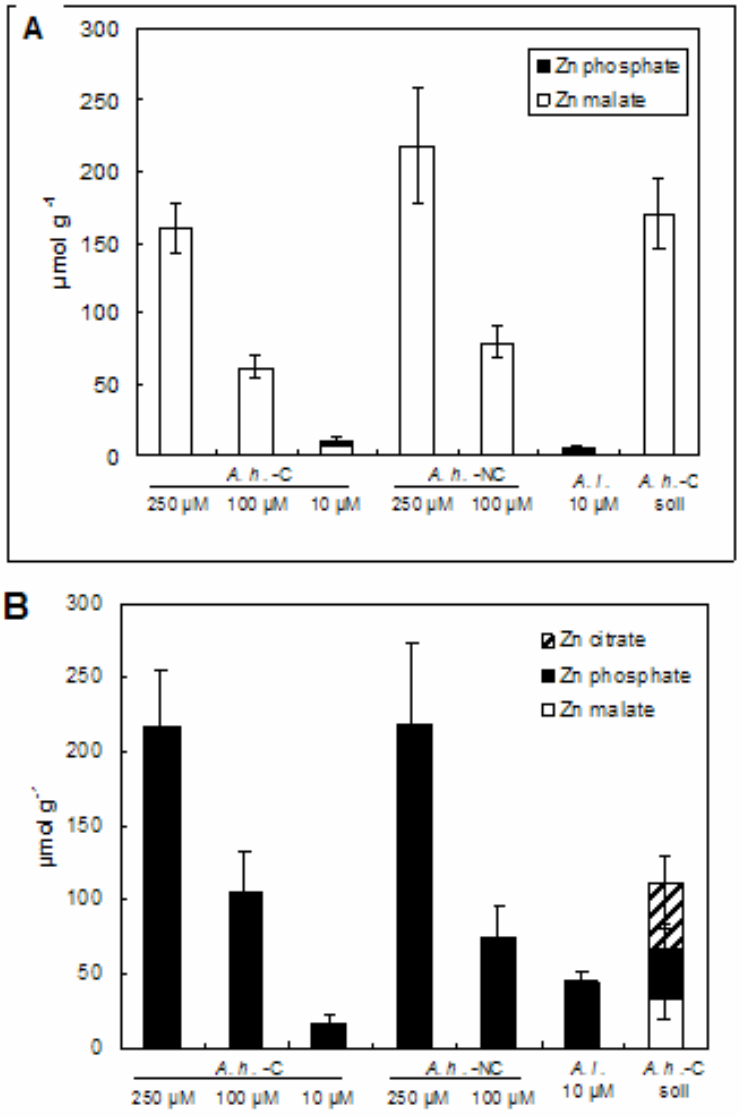

Figure 4. Concentration of Zn species in the aerial parts (A) and in the roots (B) of the plants calculated from EXAFS fitting percentages and Zn concentrations, as explained in Table II.

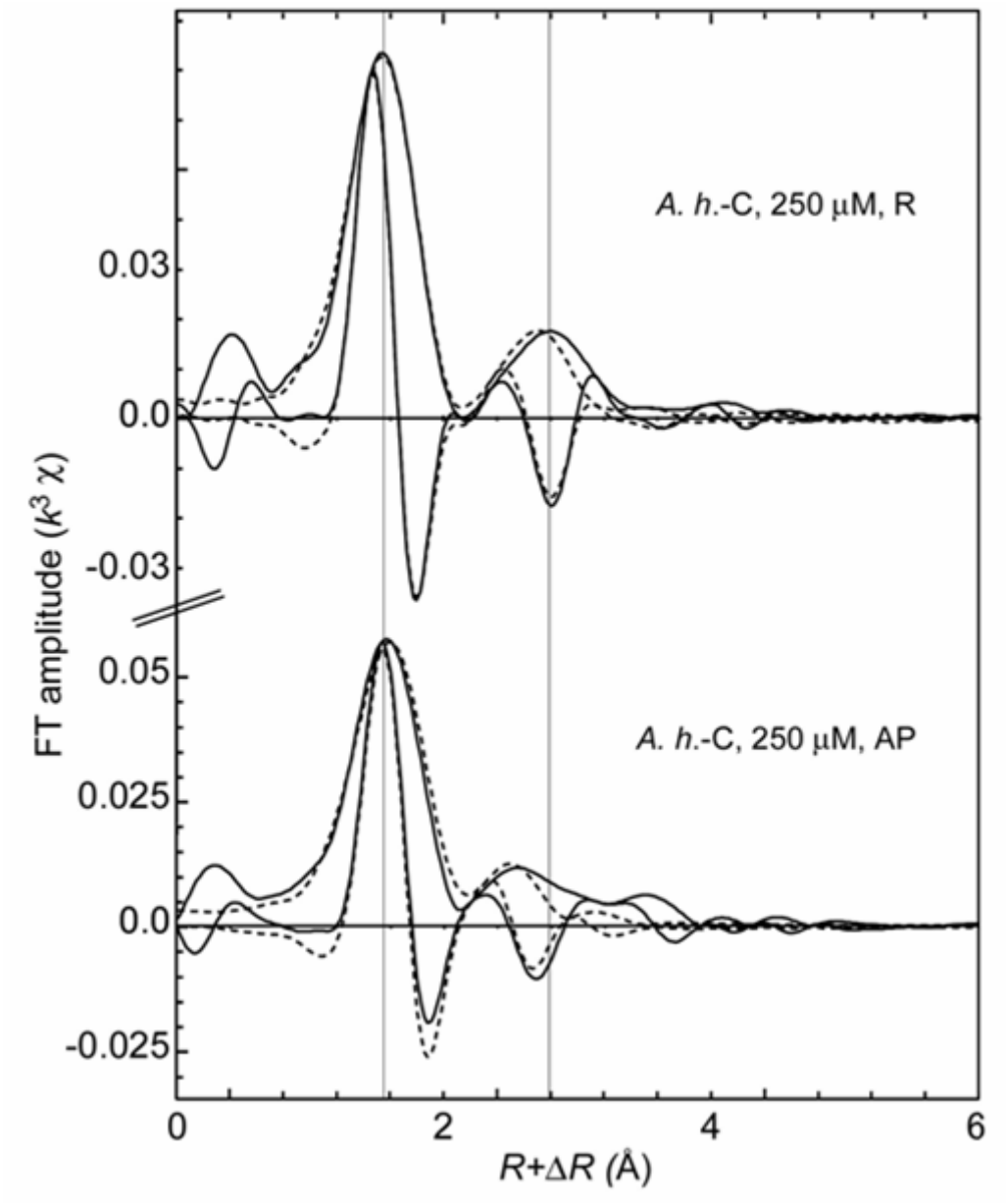

Figure 5. Radial distribution functions (modulus and imaginary part) for the roots and the aerial parts of *A. halleri* (contaminated origin) grown in solution containing 250 µM Zn. Solid lines are data and dashed lines are numerical simulations. EXAFS parameters are given in Table III.

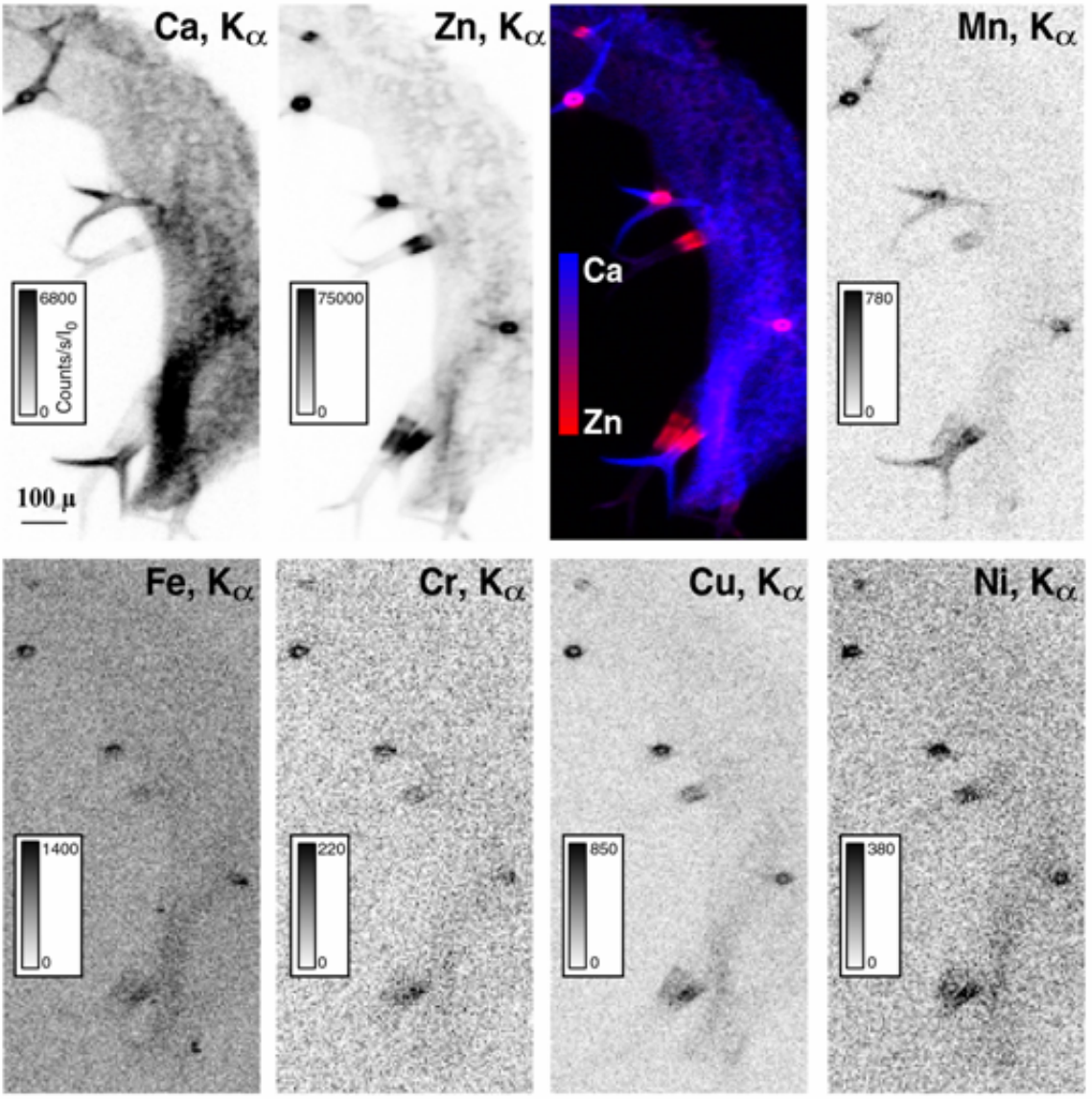

Figure 6. µSXRF elemental maps of a leaf fragment (incident beam energy: 9.7 KeV, beam size and pixel size: 5*5 µm, dwell time: 150 ms/pixel). The number of fluorescence-yield counts were normalized by I0 and the dwell time. Metals are concentrated in the bases of the trichomes.

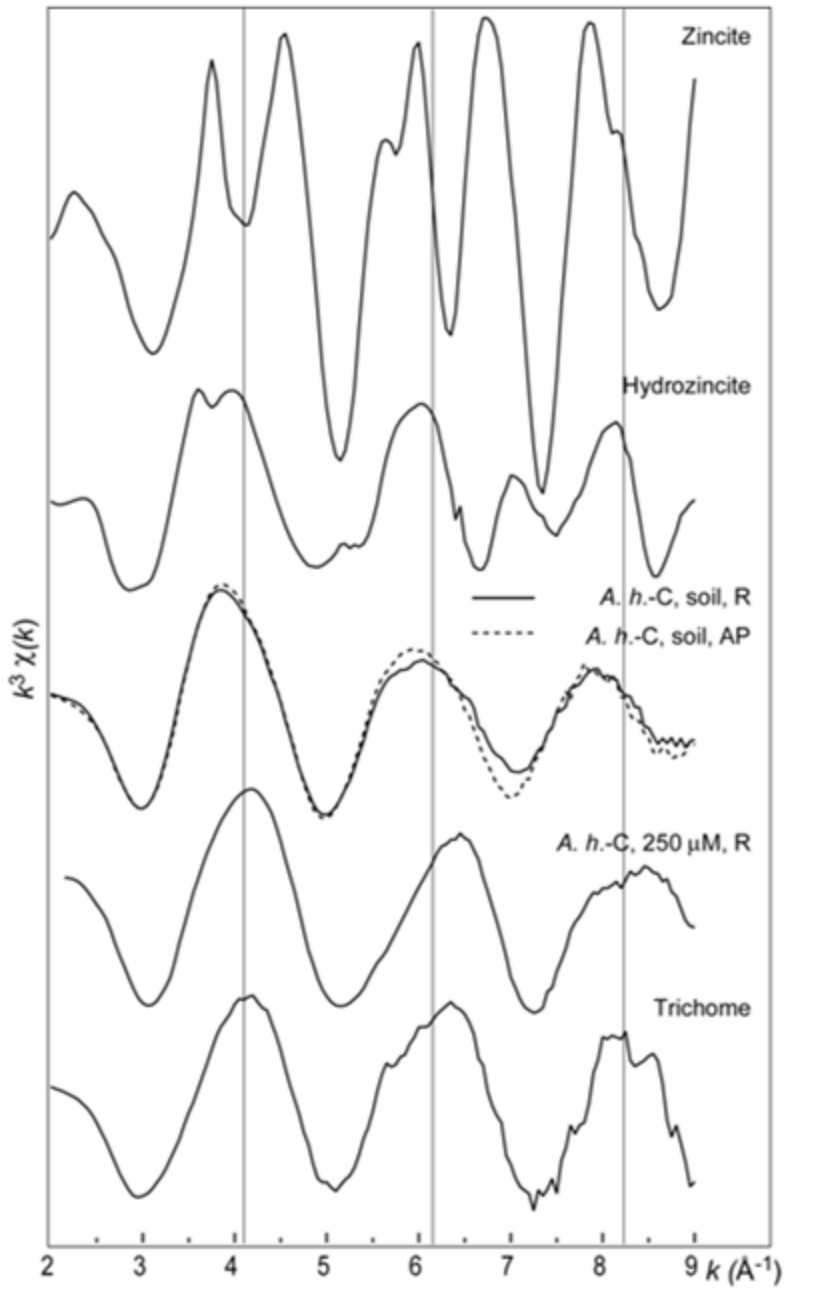

Figure 7. Comparison of the µEXAFS spectrum for the trichome to the powder EXAFS spectra for *A. h.* -C (*Arabidopsis halleri*, contaminated origin) and for a selection of reference compounds.

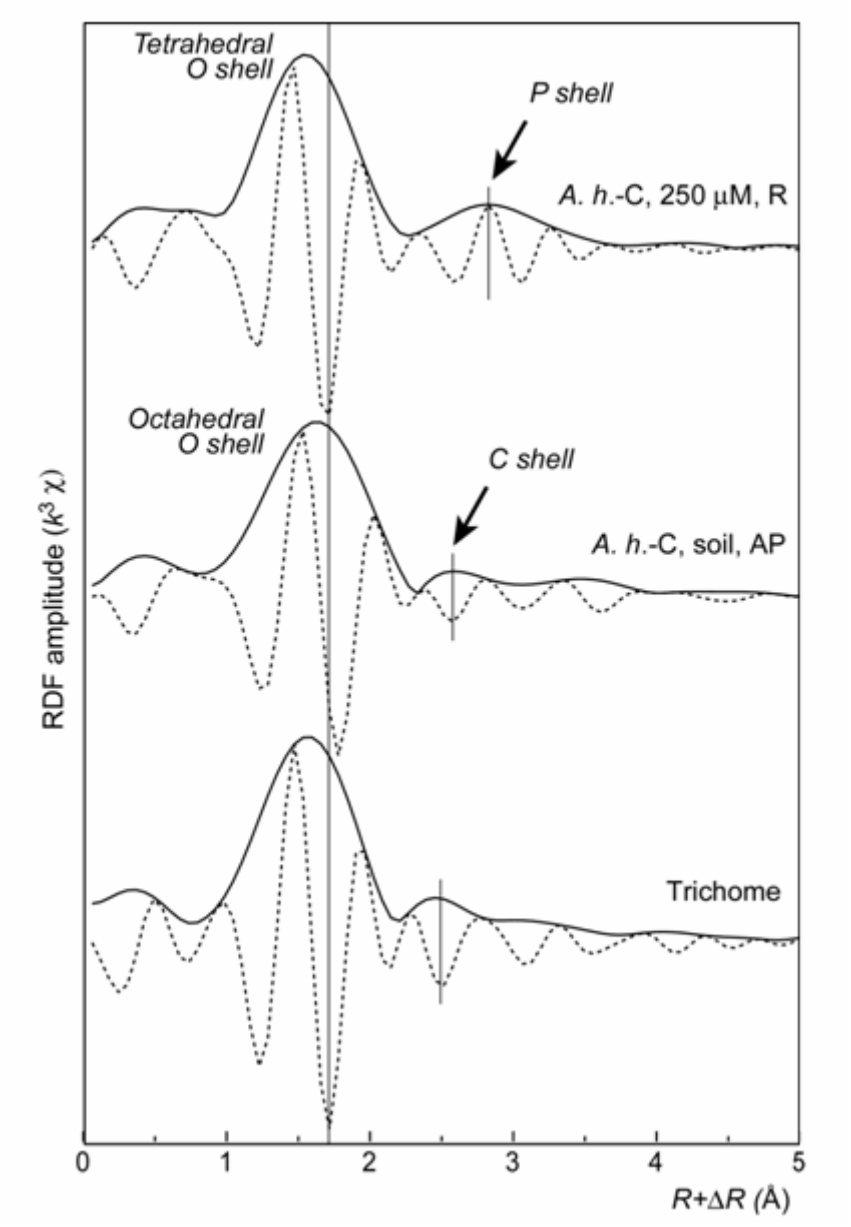

Figure 8. Radial distribution functions for the trichome and for powder samples (roots and aerial part) of *A. h.* -C (*Arabidopsis halleri*, contaminated origin).